Received: 12 April 2020 | Revised: 28 May 2020 | Accepted: 8 June 2020

DOI: 10.1111/cas.14533

ORIGINAL ARTICLE

Cancer Science WILEY

CENP-50 is required for papilloma development in the two-stage skin carcinogenesis model

Megumi Saito[1] | Naoko Kagawa[2] | Kazuhiro Okumura[1] | Haruka Munakata[1] | Eriko Isogai[1] | Tatsuo Fukagawa[2,3] | Yuichi Wakabayashi[1]

[1]Department of Carcinogenesis Research, Division of Experimental Animal Research, Chiba Cancer Center Research Institute, Chiba, Japan

[2]Department of Molecular Genetics, National Institute of Genetics and The Graduate University for Advanced Studies, Mishima, Japan

[3]Laboratory of Chromosome Biology, Graduate School of Frontier Biosciences, Osaka University, Suita, Osaka, Japan

Correspondence
Yuichi Wakabayashi, Department of Carcinogenesis Research, Division of Experimental Animal Research, Chiba Cancer Center Research Institute, Chiba, Japan.
Email: yuichi_wakabayashi@chiba-cc.jp

Funding information
Japan Society for the Promotion of Science, Grant/Award Number: 15H05972, 23790435 and 25221106

Abstract

CENP-50/U is a component of the CENP-O complex (CENP-O/P/Q/R/U) and localizes to the centromere throughout the cell cycle. Aberrant expression of *CENP-50/U* has been reported in many types of cancers. However, as *Cenp-50/U*-deficient mice die during early embryogenesis, its functions remain poorly understood in vivo. To investigate the role of *Cenp-50/U* in skin carcinogenesis, we generated *Cenp-50/U* conditional knockout (*K14Cre^{ER}-Cenp-50/U$^{fl/fl}$*) mice and subjected them to the 7,12-dimethylbenz(a)anthracene (DMBA)/terephthalic acid (TPA) chemical carcinogenesis protocol. As a result, early-stage papillomas decreased in *Cenp-50/U*-deficient mice. In contrast, *Cenp-50/U*-deficient mice demonstrated almost the same carcinoma incidence as control mice. Furthermore, mRNA expression analysis using DMBA/TPA-induced papillomas and carcinomas revealed that *Cenp-50/U* expression levels in papillomas were significantly higher than in carcinomas. These results suggest that *Cenp-50/U* functions mainly in early papilloma development and it has little effect on malignant conversion.

KEYWORDS

CENP, malignant conversion, mouse models, papilloma, two-stage skin carcinogenesis

1 | INTRODUCTION

Chromosome instability (CIN) plays a role in the multistep oncogenesis of cancer cells. CIN involves the unequal distribution of chromosomes to daughter cells upon mitosis, resulting in the loss or gain of chromosomes and/or chromosome rearrangements during cell division and, ultimately, aneuploidy. Therefore, cancer cells are characterized by aneuploidy and CIN.[1] Although CIN can be caused by multiple failures, centromere dysfunction is one of main reasons. Several studies have demonstrated a relationship between CIN and centromere dysfunction in cancer cell lines.[2-6] Overexpression of CENP-A, which is a key determinant protein for centromere formation,[7] has been found in several human malignancies, including hepatocellular carcinoma,[8,9] breast cancer[10] and ovarian cancer.[11] CENP-A expression predicts poor outcomes in patients with these cancers.

Centromere proteins are classified into several functional groups as follows: CENP-C, CENP-H/I/K/M, CENP-L/M, CENP-O/P/Q/R/U, CENP-T/W and CENP-S/X.[5,12-15] In the present study, among centromere proteins, we focused on CENP-U (CENP-50/U), which forms a complex with other CENP-O class proteins (Cenp-OO/P/Q/R/U).[16] CENP-50/U localizes to the centromere throughout the cell cycle and has been described as KLIP1/MLF1IP.[17-19]

As the centromere is essential for chromosome segregation during cell division, disruption of most centromere proteins in mice can cause embryonic lethality, accompanied by enlarged nuclei containing an increased number of nucleoli, nuclear bridging, chromosome condensation and spindle fiber bundling. For example, *Cenp-c* null mutation results in embryonic lethality at 3.5 d, with a chromosome missegregation phenotype and mitotic arrest.[20,21] *Cenp-a* null mice fail to survive beyond 6.5 d post-conception, whereas heterozygous knockout mice are healthy and fertile.[22] Therefore, it is difficult to generate centromere protein-deficient mice. As this lethality is caused by a chromosome segregation defect, cultured cells with knockout of centromere proteins should be lethal. However, we demonstrated that chicken DT40 cells with knockout of each CENP-O complex protein were viable,[16,17] (Table S1), suggesting that cells with knockout of the CENP-O complex proteins were good models to study CIN. Next, we attempted to generate centromere protein-deficient cells and demonstrated that *Cenp-r* knockout mice were viable,[23] (Table S1). Conversely, *Cenp-50/U*-deficient mouse ES cells died after they exhibited abnormal mitotic behavior, unlike the chicken DT40 cells.[24] In addition, *Cenp-50/U*-deficient mice died during early embryogenesis (at approximately E7.5),[24] (Table S1). Although these results were unexpected, the phenotype of cells with knockout of CENP-O complex proteins was weak compared with cells with other centromere proteins knocked out. Therefore, in this study, we generated *Cenp-50/U* conditional knockout mice and characterized their function related to carcinogenesis.

We have demonstrated previously the essential role of Cenp-r, which forms a complex with other Cenp-O proteins (Cenp-O/P/Q/R/U), in the two-stage skin carcinogenesis model. Cenp-r functions as a tumor suppressor in early papilloma development, but as an oncogene at the late papilloma stage and in malignant conversion.[23] Based on this study, we hypothesized that other Cenp-O complex proteins function in skin carcinogenesis. We therefore generated *K14(Keratin 14)Cre^{ER}-Cenp-50/U$^{fl/fl}$* mice to investigate the function of *Cenp-50/U* in vivo, especially in the process of carcinogenesis.

It has been shown previously that the pathology of the two-stage chemically induced skin carcinogenesis mouse model is almost identical to the development of human skin cancers, and therefore it is an ideal model to study skin cancer initiation and growth.[25,26] In the first step of this chemically induced carcinogenesis protocol, mice were treated with a low dose of the mutagen 7,12-dimethylbenz(a)anthracene (DMBA) to start tumor development. This first chemical treatment step led to "tumor initiation." In the second step, mice were treated continuously with TPA to stimulate epidermal tumor proliferation. This second chemical treatment step influenced "tumor promotion." During tumor promotion, benign tumors, known as papillomas, are thought to develop from additional mutations caused by TPA chemical treatment. After prolonged treatment (~20 wk), some papillomas will progress into carcinogenic tumors such as squamous cell carcinomas (SCC). The roles of numerous genes and cell-signaling pathways in skin tumor development could be explored with this two-stage skin carcinogenesis model using genetically engineered mouse models.[27-33]

In this study, we demonstrated the function of *Cenp-50/U* in the epidermis and its role in two-stage skin carcinogenesis. We clarified the effects of *Cenp-50/U* deficiency on mouse normal epidermis and its oncogenic role in papillomagenesis.

2 | MATERIALS AND METHODS

2.1 | Mice

This study was carried out in strict accordance with the recommendations in the Guide for the Care and Use of Laboratory Animals of the Ministry of Education, Culture, Sports, Science, and Technology of Japan. The protocol was approved by the Committee on the Ethics of Animal Experiments of Chiba Cancer Center (Permit Number: 13-18). All efforts were made to minimize suffering. C57BL/6 strain mice were used as recipients for targeted ES cells and as the background strain in this study. The generation of mice carrying the floxed allele of the *Cenp-50/U* gene (*Cenp-50/U$^{fl/fl}$*) is described elsewhere.[24] *Cenp-50/U$^{fl/fl}$* mice were mated to K14-Cre^{ER} transgenic mice.[38] K14-Cre^{ER} transgenic mice were obtained from the Jackson Laboratory (JaX 005107). To disrupt *Cenp-50/U*, K14Cre^{ER}-*Cenp-50/U$^{fl/fl}$* and *Cenp-50/U$^{fl/fl}$* mice at 8 wk old were injected subcutaneously 5 times with 1.0 mg/mL of tamoxifen (Sigma-Aldrich) that had been prepared following the manufacturer's instructions by completely dissolving tamoxifen into 1 mL of 100% ethanol at 50°C, adding 9 mL of sunflower oil and mixing this thoroughly by vortexing.

2.2 | Skin carcinogenesis

7,12-Dimethylbenz(a)anthracene (DMBA) was purchased from Sigma-Aldrich, Merck Millipore and TPA was purchased from Calbiochem, Merck Millipore. DMBA is used as a carcinogen and TPA as a promoter. At 8-10 wk of age, the backs of the mice were carefully shaved with electric clippers. At 2 d after shaving, DMBA (25 μg per mouse in 200 μL of acetone) was applied to shaved dorsal back skin. Then, 3 d after the first DMBA treatment, TPA (10 μg per mouse in 200 μL of acetone) was applied. After 4 rounds of this single DMBA and TPA treatment, the mice were treated with TPA twice weekly for 20 wk. The papilloma number and size (mm in diameter) were recorded from 8 wk up to 20 wk, and carcinoma development was monitored up to 34 wk.

2.3 | RT-PCR and quantitative real-time RT-PCR

Total RNA was isolated from normal skins, papillomas, carcinomas and metastatic carcinomas of mice after 40 wk of DMBA/TPA treatment using TRIzol (Invitrogen) in accordance with the manufacturer's protocol. cDNA was generated with the iScript™ Select cDNA Synthesis Kit (Bio-Rad) using 100 ng of DNase-pretreated total RNA. RT-PCR was performed using the Prime *Taq*

DNA Polymerase Kit (Genet Bio). The products were subjected to agarose gel electrophoresis. *Gapdh* was used as a control. qRT-PCR was performed using GeneAce SYBR® qPCR Mix α Low ROX following the manufacturer's protocol (NIPPON GENE). mRNA expression levels were measured using the Applied Biosystems® 7500 system (Life Technologies) and normalized to the levels of *Gapdh*. The following primers were used to generate *Cenp-50/U*: Forward Primer; TCT ACG CAG AAG ACG AGC TG and Reverse Primer; GTT GCT GTG ACC TTG GTC CT, *Cenp-r*: Forward Primer; CAC AGA AAC GGA CCA TCA AA and Reverse Primer; AGT TGT CTG TTG CCC TCC AA, *Cenp-o*: Forward Primer; AGA ACT GCG GCA ACA ACG and Reverse Primer; ACG ACT GGT CAA CTT CCC, *Cenp-p*: Forward Primer; ATC AGG AAA TTG CAA CAT GG and Reverse Primer; TTC GGA AAA ACA TGA GCA AA, *Cenp-q*: Forward Primer; GGA TTT GCC AGA GAA TGA GG and Reverse Primer; GAG GTT GCC AGG TTG TTC TC, and *Gapdh*: Forward Primer; TGC GAC TTC AAC AGC AAC TC and Reverse Primer; CTT GCT CAG TGT CCT TGC TG.

2.4 | Cell cycle analysis

Mouse keratinocyte cells were isolated from *Cenp-50/U*$^{fl/fl}$ and K14Cer^{ER}- *Cenp-50/U*$^{fl/fl}$ mice. Isolation of keratinocyte cells from mice was performed as described previously.[39] These were then collected and fixed in 70% ethanol at 4°C for 30 min. The fixed cells were stained with propidium iodide (50 μg/mL) containing 200 μg of RNaseA/mL and 1% Triton X-100 at 37°C for 40 min. Flow cytometry analysis was conducted using a JSAN instrument (Japan-made sorter, analyzer) (Bay Bioscience). Approximately 1.0×10^5 cells were scanned to analyze the DNA content. Necrotic cells were excluded, and the percentages of cells in the G_1, S and G_2/M phases of the cell cycle were measured.

2.5 | Immunoblotting

Proteins were extracted from different cells using T-PER Protein Extraction Reagent (Thermo). Protein concentrations were quantified by the Quick Start Bradford Protein Assay (Bio-Rad). Denatured proteins (Mouse normal skins: 60 μg) were then analyzed using 15% e-PAGELs (ATTO). After electrophoresis, these were transferred onto a polyvinylidene difluoride (PVDF) membrane (Merck Millipore). The membrane was blocked with 0.5% skimmed milk or 1% BSA in phosphate-buffered saline solution (pH 7.6) containing 0.1% Tween-20 (PBS/T) and then the SNAPi.d. 2.0 Protein Detection system (Merck Millipore). Primary antibodies were as follows: anti-Cenp-50/U (anti-rabbit polyclonal),[17] anti-Actin (Sigma-Merck Millipore). HRP-conjugated secondary antibodies were used at a dilution of 1:2000 and developed using the ECL Prime Western Blotting Detection Kit (GE Healthcare). Exposure for chemiluminescent samples or membrane analysis for the blots was performed with a LAS 4000 system (GE Healthcare).

2.6 | Immunofluorescence

Samples were fixed with 4% paraformaldehyde at 4°C overnight. The endogenous peroxidase activity in the specimens was blocked by treatment with 0.3% H_2O_2 and samples were then rinsed with PBS. Sections were incubated with primary antibodies against anti-Ki67 (1:100 16A8, Biolegend) and anti-keratin 14 (1:500 Poly19053, Biolegend) diluted in blocking buffer overnight at 4°C. Secondary antibodies were Alexa Fluor 488-conjugated anti-rat antibody (1:100, Molecular Probes, Invitrogen) and Alexa Fluor 568-conjugated anti-rabbit antibody (1:100, Molecular Probes, Invitrogen). Nuclei were counterstained with Hard Set Mounting Medium with DAPI (Vector). All fluorescence images were obtained on a Leica TCS SPE confocal microscope equipped with a DMI400B (×10/0.40, ×20/0.70 and ×40/1.25 oil immersion objectives).

2.7 | TUNEL staining

Apoptotic scores were obtained by terminal deoxynucleotidyl transferase dUTP nick end labeling (TUNEL) assay using an in situ Apoptosis Detection Kit (TaKaRa). Samples were digested with proteinase K (20 μg/mL) and labeled with TUNEL reaction mixture for 90 min at 37°C. All images were obtained on a Leica TCS SPE confocal microscope equipped with a DMI400B (×10/0.40, ×20/0.70 and ×40/1.25 oil immersion objectives). Data from all fields and all samples were pooled to obtain the apoptotic index, which was the percentage of TUNEL-positive cells of total cells manually counted in randomly selected fields, and compared between *Cenp-50/U*$^{fl/fl}$ and K14Cer^{ER}- *Cenp-50/U*$^{fl/fl}$ mice.

2.8 | Statistical analysis

At least 3 replicates were performed for all experiments. The significance of differences was calculated using unpaired one- and two-tailed Student *t* tests or two-way ANOVA. A *P*-value < .05 was considered significant and a value < .01 was highly significant. These analyses were performed using GraphPad Prism software (GraphPad).

3 | RESULTS

3.1 | mRNA expression profiles of the *Cenp-O* complex are altered in skin tumors

First, we examined mRNA expression levels of *Cenp-O* complex (*Cenp-O/P/Q/R/U*) genes using DMBA/TPA-induced papillomas (n = 10) and carcinomas (n = 10). As a result, *Cenp-50/U* and *Cenp-r* expression levels differed between papillomas and carcinomas (Figure 1A,B). Conversely, *Cenp-o*, *Cenp-p* and *Cenp-q* had the

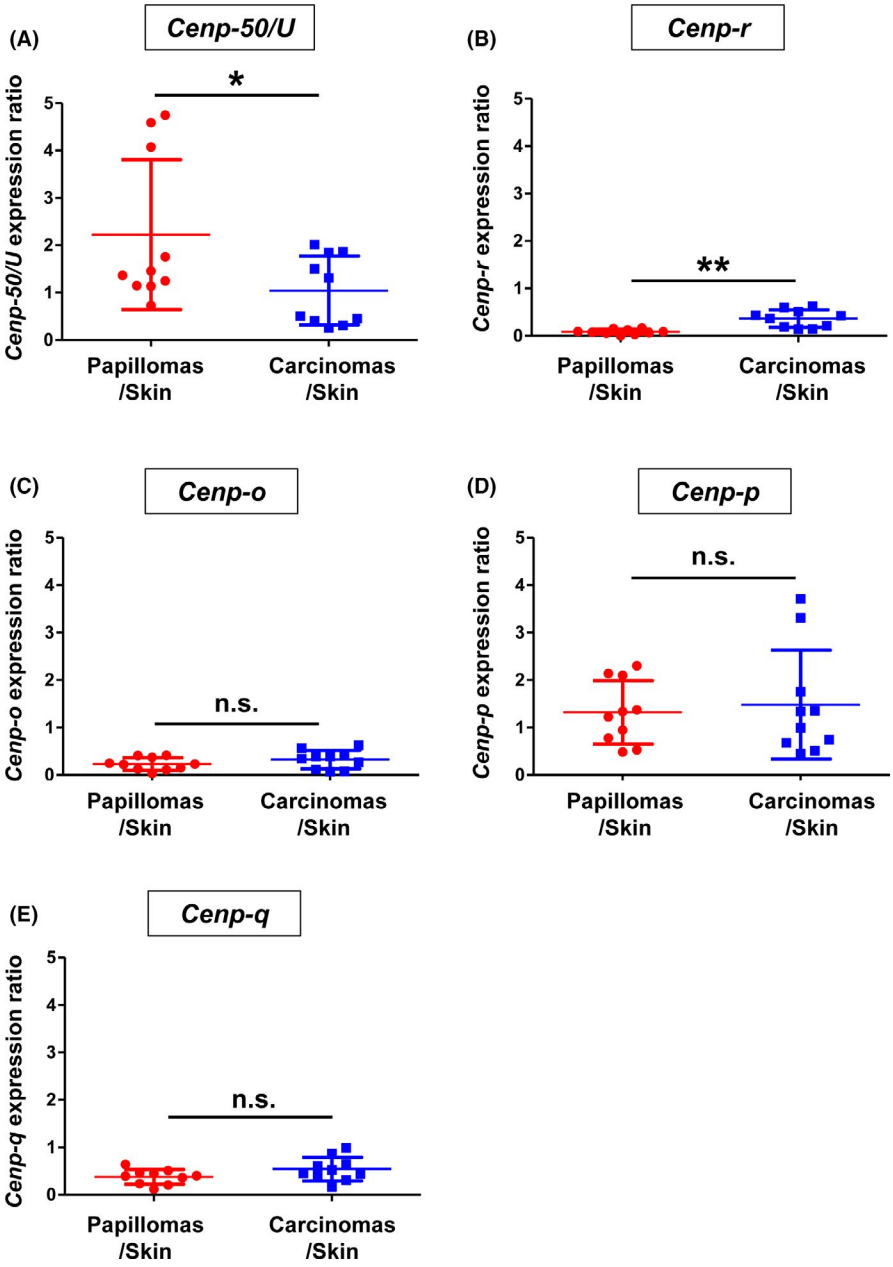

FIGURE 1 The CENP-O family is expressed differently in skin tumors. mRNA expression levels in skin tumors (Papillomas/Skin (red) (n = 10), Carcinomas/Skin (blue) (n = 10)). mRNA expression levels detected by qRT-PCR. A, *Cenp-50/U* ($P = .0253$). B, *Cenp-r* ($P = .00140$). C, *Cenp-o* ($P = .255$). D, *Cenp-p* ($P = .771$) and E, *Cenp-q* ($P = .212$). These expression levels were normalized by *Gapdh* in skins, papillomas and carcinomas first and then the ratios between papillomas and skins and between carcinomas and skins are presented. The *P*-values were calculated by two-way ANOVA (**$P < .01$; *$P < .05$). n.s., not significant. Error bars represent the standard deviation (SD)

same expression levels in papillomas and carcinomas (Figure 1C-E). These results suggested that *Cenp-50/U* and *Cenp-r* are more likely to be involved in skin carcinogenesis than *Cenp-o*, *Cenp-p* and *Cenp-q*.

Cenp-r expression levels in carcinomas were significantly higher than in papillomas (Figure 1B). In contrast, *Cenp-50/U* expression levels in carcinomas were significantly lower than in papillomas (Figure 1A). In other words, *Cenp-50/U* and *Cenp-r* exhibited opposite expression profiles in skin carcinogenesis. Our previous study revealed that *Cenp-r* functions as a tumor suppressor-type gene in papilloma development and as an oncogene-type gene during the progression stage.[23] These results suggested that *Cenp-50/U* plays a opposing role to *Cenp-r* in skin carcinogenesis.

3.2 | Generation of *Cenp-50/U* conditional knockout mice

A previous study demonstrated that *Cenp-50/U* knockout mice die during early embryogenesis (approximately E7.5).[24] To investigate the function of *Cenp-50/U* in vivo, we generated mice harboring conditional alleles of *Cenp-50/U*, in which exons 4-6 of the *Cenp-50/U* gene are flanked by *loxP* sites (Figure 2A). First, we isolated mice with *Cenp-50/U*$^{fl/+}$ alleles and finally generated *Cenp-50/U*$^{fl/fl}$ alleles by intercrossing (Figure 2B). Next, we crossed the *Cenp-50/U*$^{fl/fl}$ conditional knockout mice with mice carrying a *K14Cre*^{ER} allele,[34] which is specifically expressed in the epidermis, to generate *K14Cre*^{ER}-*Cenp-50/U*$^{fl/fl}$ progeny in which *Cenp-50/U* can be rendered non-functional in the skin upon induction with tamoxifen.

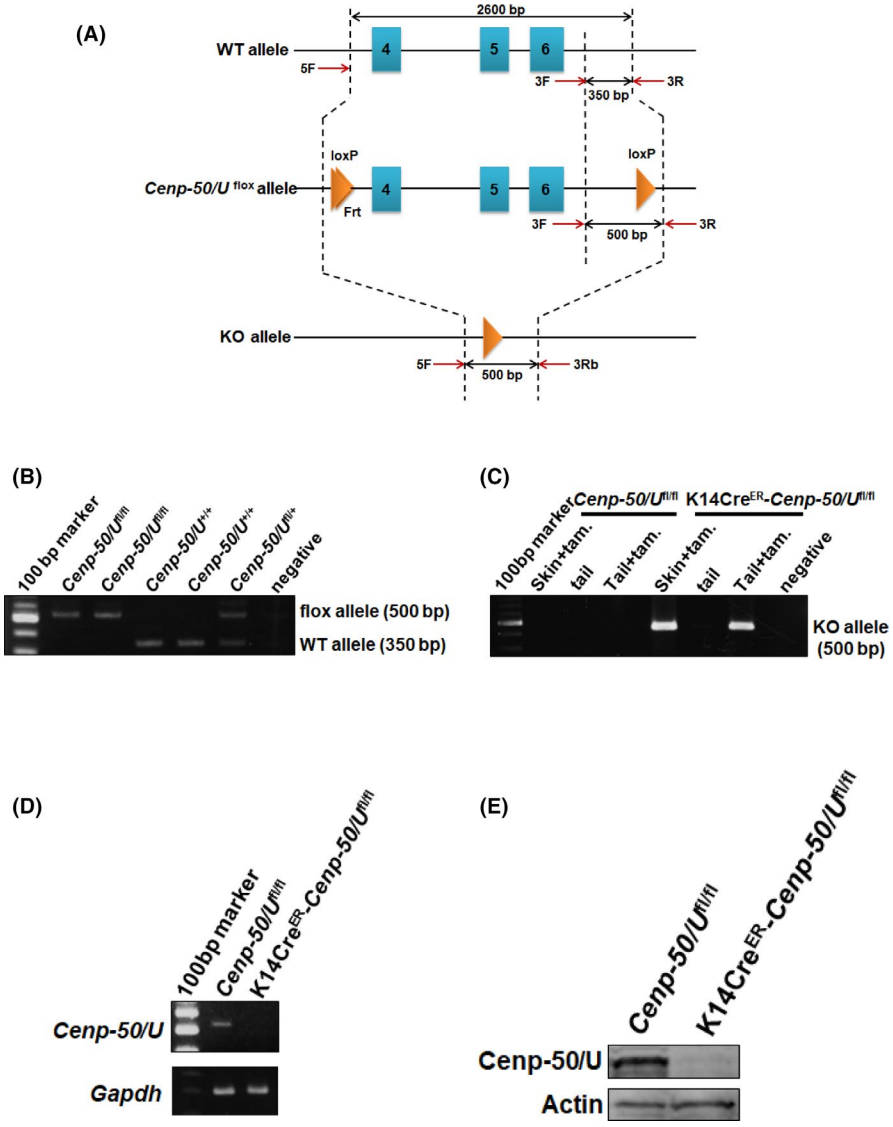

FIGURE 2 Generation of *Cenp-50/U* knockout mice. A, Targeting strategy to generate mice lacking *Cenp-50/U*. Blue boxes indicate the positions of exons. loxP was inserted into the genomic region in exons 4-6 of the *Cenp-50/U* gene. Red arrows indicate the construction primers for detection of the *Cenp-50/U*$^{fl/fl}$-allele and *Cenp-50/U* knockout allele. B, Genotype analysis of genomic DNA from *Cenp-50/U*$^{fl/fl}$ mice. The floxed allele and wild-type allele were detected by 3F and 3R primers (floxed allele: approximately 500 bp, wild-type allele: 350 bp). C, Genotype analysis of *Cenp-50/U* knockout (KO) allele. The KO allele was detected by 5F and 3Rb primers (approximately 500 bp) using genomic DNA from mouse skins and tail. D, *Cenp-50/U* expression levels detected by RT-PCR. RT-PCR analysis using mouse skins from *Cenp-50/U*$^{fl/fl}$ and K14Cer^{ER}- *Cenp-50/U*$^{fl/fl}$ mice. *Gapdh* expression is shown as an internal control. E, Cenp-50/U protein expression levels measured by western blot analysis using mouse skins from *Cenp-50/U*$^{fl/fl}$ and K14Cer^{ER}-*Cenp-50/U*$^{fl/fl}$ mice. Actin expression is shown as an internal control

Five subcutaneous injections of tamoxifen into *K14Cre*^{ER}-*Cenp-50/U*$^{fl/fl}$ mice was sufficient to disrupt the floxed *Cenp-50/U* locus in the dorsal back skin and tail (Figure 2C). In addition, we examined Cenp-50/U expression levels in *K14Cre*^{ER}-*Cenp-50/U*$^{fl/fl}$ and *Cenp-50/U*$^{fl/fl}$ mice after subcutaneous injection with tamoxifen. As a result, mRNA expression and protein of Cenp-50/U was not detected in *K14Cre*^{ER}-*Cenp-50/U*$^{fl/fl}$ mouse skins by RT-PCR and western blot analyses with anti-Cenp-50/U antibody, respectively (Figure 2D,E).

3.3 | *Cenp-50/U* deficiency affects cell proliferation in normal skins

As we successfully generated epidermis-specific *Cenp-50/U* knockout mice, we investigated the function of *Cenp-50/U* in the epidermis using these mice. First, we performed histological analysis using skins from *K14Cre*^{ER}-*Cenp-50/U*$^{fl/fl}$ and *Cenp-50/U*$^{fl/fl}$ mice after subcutaneous injection with tamoxifen. Hematoxylin-eosin (HE) staining revealed no significant morphological changes (Figure S1A,B). We then carried out immunohistochemical analysis with the cell proliferation marker Ki67 and TUNEL staining to investigate apoptotic cells in skins. As a result, skins from *K14Cre*^{ER}-*Cenp-50/U*$^{fl/fl}$ mice had a significantly lower number of Ki67-positive cells than skins from *Cenp-50/U*$^{fl/fl}$ mice (Figure 3A,B,E). Conversely, TUNEL-positive cells were detected in *K14Cre*^{ER}-*Cenp-50/U*$^{fl/fl}$ mouse skins, although they were not detected in *Cenp-50/U*$^{fl/fl}$ mouse skins (Figure 3C,D,F). However, only a few TUNEL-positive cells per field were detected in *K14Cre*^{ER}-*Cenp-50/U*$^{fl/fl}$ mouse skins. To confirm these results, we performed cell cycle analysis. The percentage of cells in the G_0/G_1 phase was significantly lower in skins of *K14Cre*^{ER}-*Cenp-50/U*$^{fl/fl}$ mice than in those of *Cenp-50/U*$^{fl/fl}$ mice (Figure 3G). In addition, the percentage of cells in the subG$_1$ phase was significantly higher in skins of *K14Cre*^{ER}-*Cenp-50/U*$^{fl/fl}$ mice than in those of *Cenp-50/U*$^{fl/fl}$ mice (Figure 3G). However, we did not observe accumulation of G2/M phase in skins of *K14Cre*^{ER}-*Cenp-50/U*$^{fl/fl}$ mice, suggesting that cells went through mitosis, even if subtle centromere

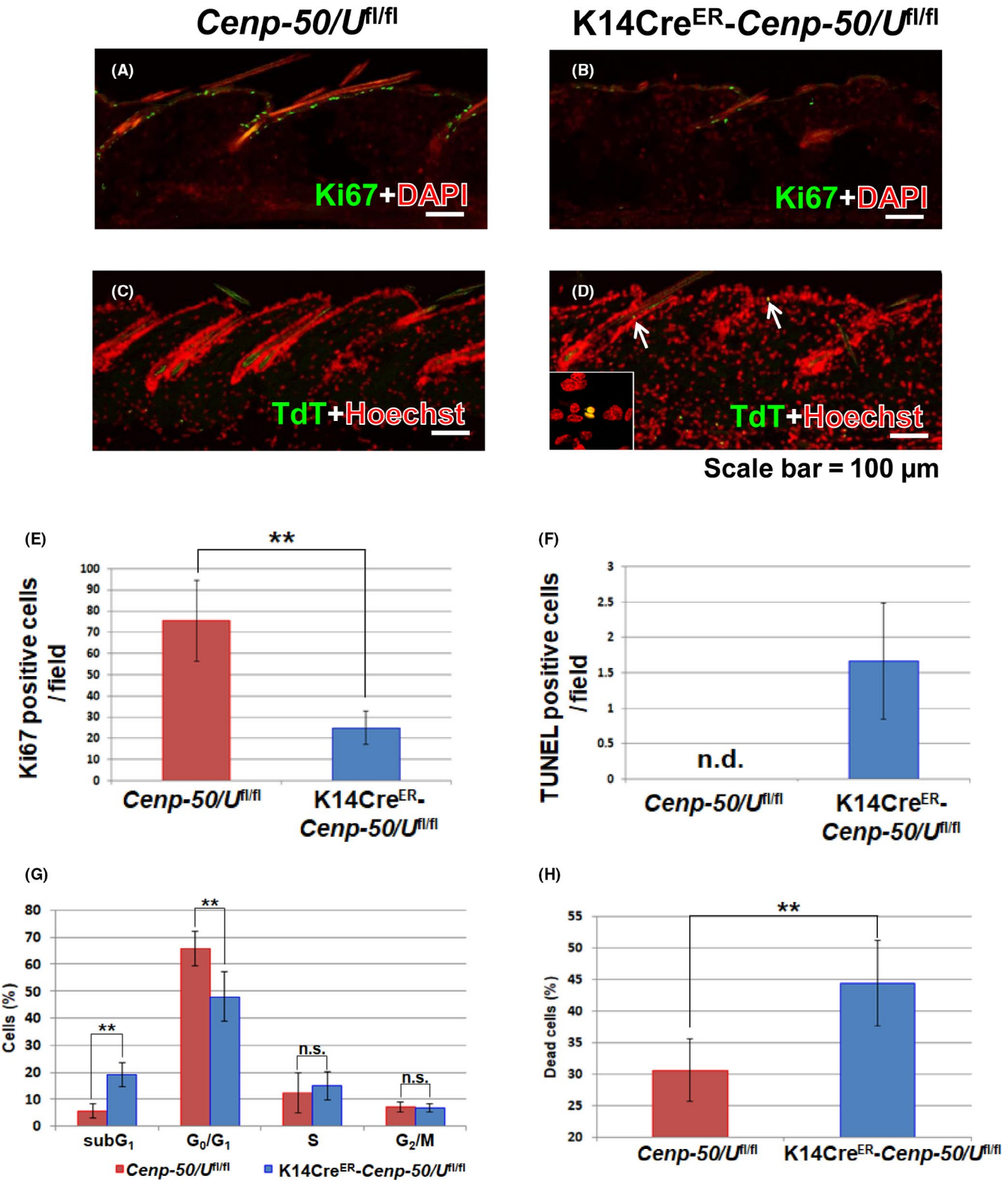

FIGURE 3 *Cenp-50/U*-deficient mice have a decrease in cell proliferation in normal skins. A, B, Immunostaining patterns of Ki67 (green) in skins from (A) *Cenp-50/U*$^{fl/fl}$ and (B) K14Cer^{ER}-*Cenp-50/U*$^{fl/fl}$ mice. C, D, Representative TUNEL staining pattern of TdT (green) in skins from (C) *Cenp-50/U*$^{fl/fl}$ and (D) K14Cer^{ER}-*Cenp-50/U*$^{fl/fl}$ mice. Cells were counterstained with Hoechst (red). E, The number of Ki67-positive cells in skins from *Cenp-50/U*$^{fl/fl}$ (n = 12) (red bar) and K14Cer^{ER}-*Cenp-50/U*$^{fl/fl}$ (n = 12) (blue bar) mice (P = 4.93E-8). F, The number of TUNEL-positive cells in skins from *Cenp-50/U*$^{fl/fl}$ (n = 7) and K14Cer^{ER}-*Cenp-50/U*$^{fl/fl}$ mice (n = 7) (blue bar). G, Cell cycle analysis of mouse normal skins from *Cenp-50/U*$^{fl/fl}$ (n = 6) (red bar) and K14Cer^{ER}-*Cenp-50/U*$^{fl/fl}$ (n = 5) (blue bar) mice (G_0/G_1 phase: P = .00424, $subG_1$ phase: P = .000203). DNA content was measured by propidium iodide (PI) staining. H, Trypan blue exclusion test of cell viability. Cells were isolated from *Cenp-50/U*$^{fl/fl}$ (n = 6) (red bar) and K14Cer^{ER}-*Cenp-50/U*$^{fl/fl}$ (n = 5) (blue bar) mice (P = .002013). The P-value was calculated by t test (**P < .01). n.s., not significant. n.d., not detected. Error bars represent the standard deviation (SD)

dysfunctions happened. We also performed the trypan blue exclusion test of cell viability using cells isolated from skins of *K14Cre*^{ER}-*Cenp-50/U*$^{fl/fl}$ and *Cenp-50/U*$^{fl/fl}$ mice. As a result, the percentage of dead cells was significantly higher in skins of *K14Cre*^{ER}-*Cenp-50/U*$^{fl/fl}$ mice than in those of *Cenp-50/U*$^{fl/fl}$ mice (Figure 3H). These results suggested that *Cenp-50/U* deficiency promotes cell death by apoptosis and reduces cell proliferation in mouse skins.

3.4 | *Cenp-50/U* deficiency partially inhibits papillomagenesis

Our previous study demonstrated the essential function of Cenp-r in the two-stage skin carcinogenesis model.[23] In this study, our expression analysis suggested that Cenp-50/U functions might be opposite to those of Cenp-r in skin carcinogenesis (Figure 1). To investigate

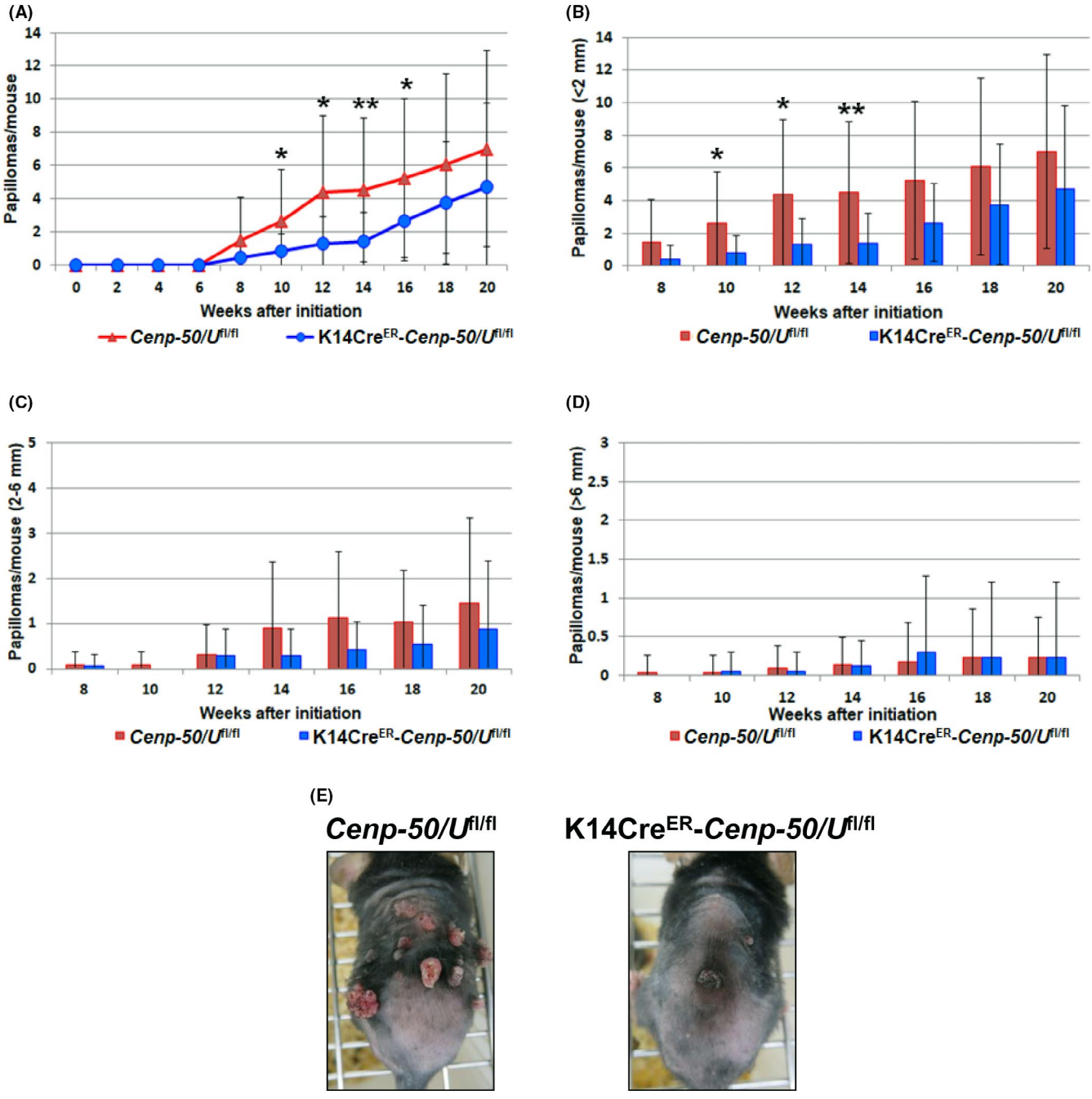

FIGURE 4 *Cenp-50/U* functions in early tumor development. A, Comparison of DMBA/TPA-induced papilloma numbers per mouse between *Cenp-50/U*$^{fl/fl}$ (n = 22) (red line) and K14Cer^{ER}-*Cenp-50/U*$^{fl/fl}$ (n = 17) (blue line) mice. B, Number of papillomas < 2 mm per mouse. C, Number of papillomas 2-6 mm per mouse. D, Number of papillomas >6 mm per mouse. Red bars represent *Cenp-50/U*$^{fl/fl}$ mice. Blue bars represent K14Cer^{ER}-*Cenp-50/U*$^{fl/fl}$ mice. E, Representative photographs of *Cenp-50/U*$^{fl/fl}$ (left) and K14Cer^{ER}-*Cenp-50/U*$^{fl/fl}$ (right) mice at 20 wk after initiation. The *P*-values were calculated by *t* test (**P < .01; *P < .05). n.s., not significant. Error bars represent the standard deviation (SD)

the role of Cenp-50/U in skin carcinogenesis, we subjected *K14Cre*^{ER}-*Cenp-50/U*$^{fl/fl}$ and *Cenp-50/U*$^{fl/fl}$ mice to the DMBA/TPA chemical carcinogenesis protocol, and papilloma development was monitored for a period of 20 wk. As a result, *K14Cre*^{ER}-*Cenp-50/U*$^{fl/fl}$ mice exhibited a significantly lower number of papillomas than *Cenp-50/U*$^{fl/fl}$ mice between 10 and 16 wk after initiation (Figure 4A,E, Table S2). In addition, we classified these papillomas into 3 categories based on size (<2, 2-6 and >6 mm). *K14Cre*^{ER}-*Cenp-50/U*$^{fl/fl}$ mice demonstrated a significant decrease only in small papillomas < 2 mm in diameter between 10 and 14 wk after initiation (Figure 4B-D, Table S2). These results suggested that *Cenp-50/U* mainly functions in early papilloma development, but has a weak effect on papilloma growth.

3.5 | *Cenp-50/U* deficiency increases apoptotic cells in papillomas

Skin carcinogenesis experiments revealed that Cenp-50/U functions in early papilloma development. Therefore, we investigated cell proliferation and apoptosis in papillomas of *K14Cre*^{ER}-*Cenp-50/U*$^{fl/fl}$ and *Cenp-50/U*$^{fl/fl}$ mice. First, we performed histological analysis using early-stage papillomas (<6 mm) from *K14Cre*^{ER}-*Cenp-50/U*$^{fl/fl}$ and *Cenp-50/U*$^{fl/fl}$ mice. As HE staining revealed no significant morphological changes between these mice (Figure S1C,D), we carried out immunohistochemical analysis with the cell proliferation marker Ki67 and TUNEL staining to investigate apoptotic cells in papillomas. Papillomas of *K14Cre*^{ER}-*Cenp-50/U*$^{fl/fl}$ mice had a significantly higher number of TUNEL-positive cells than those of *Cenp-50/U*$^{fl/fl}$ mice (Figure 5C,D,F). Conversely, no significant difference between *K14Cre*^{ER}-*Cenp-50/U*$^{fl/fl}$ and *Cenp-50/U*$^{fl/fl}$ mice was observed by immunohistochemical analysis with the cell proliferation marker Ki67 (Figure 5A,B,E). Therefore, *Cenp-50/U* deficiency promotes cell death by inducing apoptotic cells rather than controlling cell proliferation in papillomas. These finding are consistent with previous reports, which stated that *CENP-50/U*-deficient DT40 cells undergo apoptosis.[17] Therefore, Cenp-50/U regulates abnormal mitosis both in mice and cell lines.

3.6 | Cenp-50/U is required for early papilloma development, but has little effect on malignant conversion

To investigate the effects of Cenp-50/U on malignant conversion, we monitored carcinoma development up to 34 wk after initiation. The carcinoma incidence was almost the same in *K14Cre*^{ER}-*Cenp-50/*

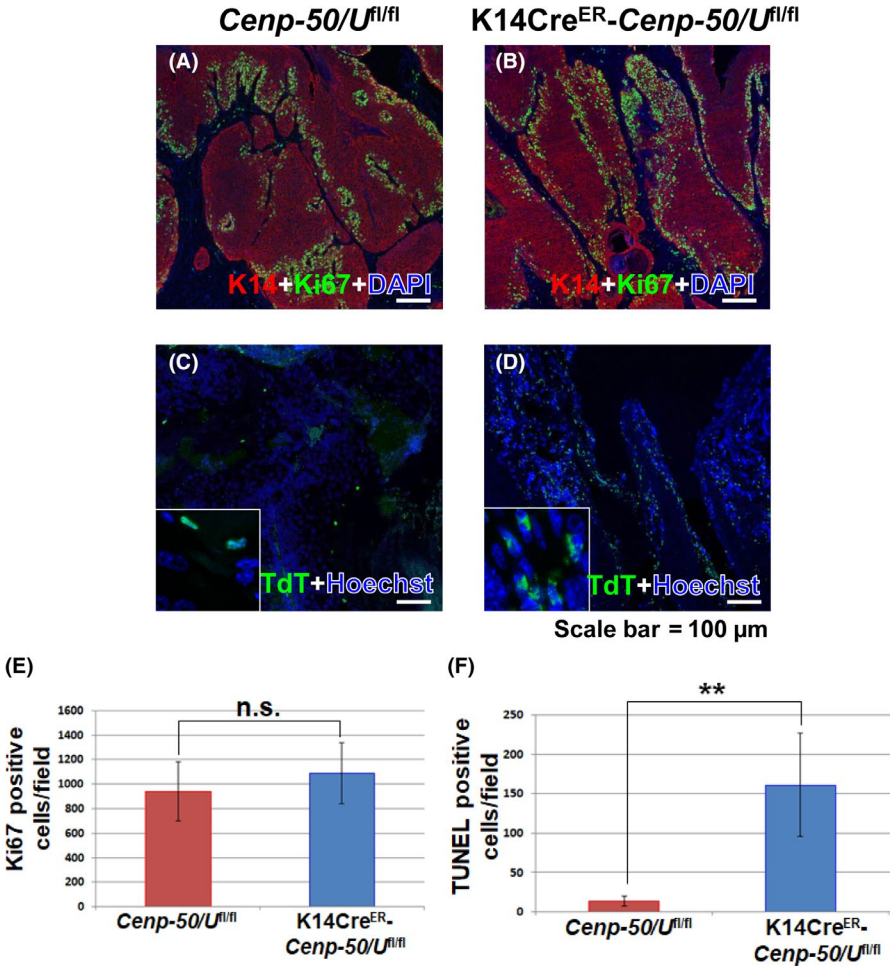

FIGURE 5 *Cenp-50/U* deficiency induces cell death in papillomas. A, B, Immunostaining patterns of Ki67 (green) and K14 (red) in papillomas from (A) *Cenp-50/U*$^{fl/fl}$ and (B) K14Cer^{ER}-*Cenp-50/U*$^{fl/fl}$ mice. C, D, Representative TUNEL staining pattern of TdT (green) in papillomas from (C) *Cenp-50/U*$^{fl/fl}$ and (D) K14Cer^{ER}-*Cenp-50/U*$^{fl/fl}$ mice (P = .00217). Cells were counterstained with Hoechst (blue). White inset boxes indicate the magnified region. E, The number of Ki67-positive cells in papillomas from *Cenp-50/U*$^{fl/fl}$ (n = 12) (red bar) and K14Cer^{ER}-*Cenp-50/U*$^{fl/fl}$ (n = 12) (blue bar) mice (P = .144). F, The number of TUNEL-positive cells in papillomas from *Cenp-50/U*$^{fl/fl}$ (n = 8) (red bar) and K14Cer^{ER}-*Cenp-50/U*$^{fl/fl}$ (n = 8) (blue bar) mice. The P-value was calculated by t test (**P < .01). n.s., not significant. Error bars represent the standard deviation (SD)

$U^{fl/fl}$ (58.8%) and *Cenp-50/*$U^{fl/fl}$ (59.1%) mice at 34 wk after initiation (Figure 6A). In addition, malignant conversion ratio per papilloma was almost the same in *K14Cre*^{ER}*-Cenp-50/*$U^{fl/fl}$ (13.4%) and *Cenp-50/*$U^{fl/fl}$ (16.2%) mice at 34 wk after initiation (Figure 6B). We then performed histological analysis using carcinomas from *K14Cre*^{ER}*-Cenp-50/*$U^{fl/fl}$ and *Cenp-50/*$U^{fl/fl}$ mice. HE staining revealed no significant morphological changes between these mice (Fig. S1E,F). These results suggested that *Cenp-50/U* has almost no effect on malignant conversion.

In this study, we found a decrease in early-stage papillomas in *Cenp-50/U*-deficient mice due to the induction of cell death, but there was little effect on malignant conversion. Taken together, *Cenp-50/U* mainly functions in papilloma development, and does not play a role in papilloma growth or malignant conversion (Figure 7).

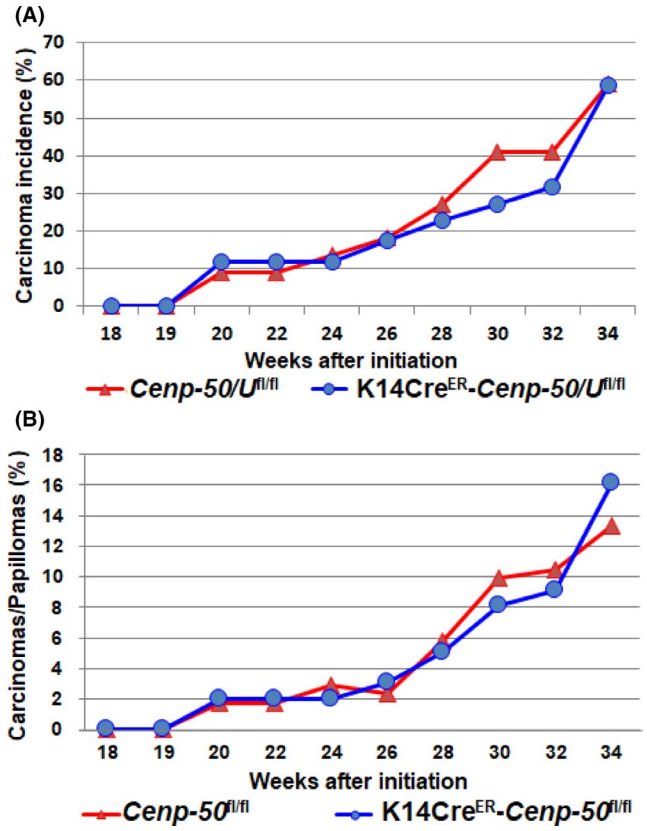

FIGURE 6 *Cenp-50/U* has little effect on malignant conversion. A, Comparison of the incidence of DMBA/TPA-induced carcinoma between *Cenp-50/*$U^{fl/fl}$ (n = 22) (red line) and K14Cre^{ER}*-Cenp-50*$^{fl/fl}$ (n = 17) (blue line) mice. B, Comparison of the incidence of DMBA/TPA-induced carcinomas per papilloma between *Cenp-50/*$U^{fl/fl}$ (n = 172) (red line) and K14Cer^{ER}*-Cenp-50/*$U^{fl/fl}$ (n = 99) (blue line) mice

4 | DISCUSSION

In this study, we specifically knocked out *Cenp-50/U* in the epidermis, and clarified its function in two-stage skin carcinogenesis. *Cenp-50/U* deficiency promoted cell death in normal mouse skins. In addition, our skin carcinogenesis experiments revealed that *Cenp-50/U* deficiency downregulates early papillomagenesis by inducing cell death.

Centromere proteins play a fundamental role in accurate chromosome segregation during mitosis and meiosis. Chromosome segregation errors cause genetic diseases, including some cancers. In addition, several centromere proteins play an important role in embryonic development.[4,20-22,35] Therefore, it was difficult to generate centromere protein-deficient mice and perform functional analysis in vivo. As *Cenp-50/U*-deficient mice also died during early embryogenesis (approximately E7.5),[24] its functions were poorly understood. Therefore, we generated *Cenp-50/U* conditional knockout mice and analyzed its function in vivo.

Cenp-50/U is a centromere protein, but unlike other centromere proteins including CENP-A or CENP-C, CENP-50/U-deficient DT40 cells are viable, suggesting that CENP-50/U-deficient DT40 cells have undergone mitosis, even if mitotic abnormalities happen.[17] However, some populations of CENP-50/U-deficient DT40 cells cause cell death through apoptosis, which is similar to that observed in *K14Cre*^{ER}*-Cenp-50/*$U^{fl/fl}$ mouse skins and papillomas. These observations suggested that Cenp-50/U is critical for cell division to ensure accurate chromosome segregation. By contrast, Cenp-50/U is dispensable in malignant conversion. In this stage, cells might tolerate abnormal mitotic cells like DT40 cells. The essentiality of

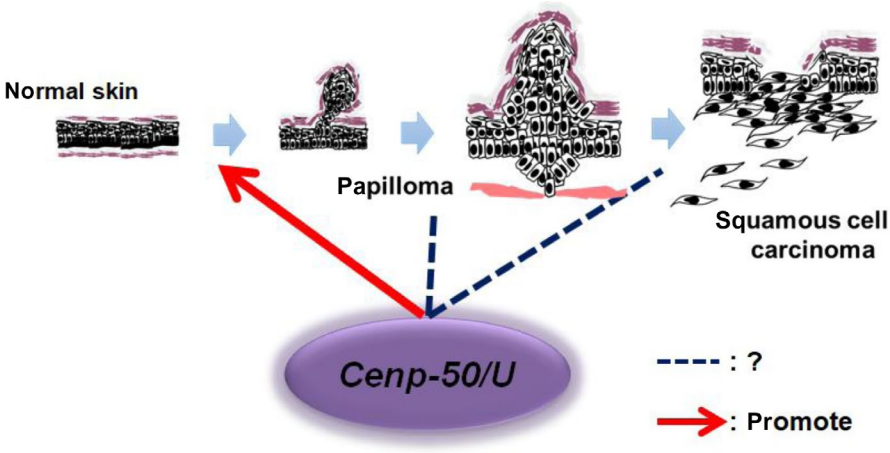

FIGURE 7 Schematic drawing of the functions of *Cenp-50/U* in the process of skin carcinogenesis. *Cenp-50/U* regulates early papilloma development. Conversely, *Cenp-50/U* has little effect on papilloma growth and malignant conversion

CENP-50/U varies between cell types and it is necessary early in papilloma growth.

Recent studies have reported aberrant expression of *CENP-50/U* in many types of cancers, including breast cancer, prostate cancer, colorectal carcinoma, ovarian cancer, glioblastoma, erythroleukemia, and lymphoma.[36,37] These might be related to variety of CENP-50/U effects in various cell types and also suggested that *CENP-50/U* is a molecular marker for cancer therapy. We demonstrated that *Cenp-50/U* is highly expressed in papillomas and is involved in the early papillomagenesis stage, and this positive correlation suggested that *Cenp-50/U* can be a molecular marker in carcinogenesis.

Our skin carcinogenesis experiments using *K14Cre^{ER}-Cenp-50/U$^{fl/fl}$* mice demonstrated that *Cenp-50/U* deficiency reduces early-stage papillomas. However, *Cenp-50/U* deficiency has little effect on malignant conversion. Consistent with this, *Cenp-50/U* is highly expressed in papilloma, but expression was decreased in malignant conversion. This finding suggests that *Cenp-50/U* functions as an oncogene in papilloma development, but loses this function at the late papilloma stage and in malignant conversion. We previously reported that *Cenp-r* deficiency increases early-stage papillomas and reduces the conversion of benign papillomas into malignant tumors.[23] These results suggest that *Cenp-50/U* functions as an oncogene, whereas *Cenp-r* functions as a tumor suppressor in early papilloma development. Furthermore, based on mRNA expression analysis, *Cenp-50/U* and *Cenp-r* exhibit opposite expression profiles in papillomas and carcinomas. Although Cenp-50/U and Cenp-r form the Cenp-O complex, these genes have different functions in the two-stage skin carcinogenesis model. Our previous study demonstrated that CENP-R localized to the centromere downstream of other CENP-O complex proteins, which can assemble a functional form in the absence of CENP-R,[16] suggesting that CENP-R plays a distinct role compared with other CENP-O complex proteins. Skin carcinogenesis experiments using mice lacking multiple CENP-O complex proteins to elucidate the molecular mechanisms need to be carried out in detail in the future.

In conclusion, we demonstrated that Cenp-50/U plays a major role in early papilloma development and is involved in cell death, including apoptosis. In addition, Cenp-R and Cenp-50/U in the Cenp-O complex have different functions in the two-stage carcinogenesis model. Cenp-50/U may function either alone or in association with other centromere proteins in carcinogenesis, potentially leading to a novel therapeutic strategy.

ACKNOWLEDGMENTS

This study was supported by JSPS KAKENHI Grant Number 23790435, 25221106 and 15H05972.

CONFLICT OF INTEREST

The authors have no conflict of interest.

ORCID

Yuichi Wakabayashi https://orcid.org/0000-0002-8861-2954

REFERENCES

1. Lengauer C, Kinzler KW, Vogelstein B. Genetic instabilities in human cancers. *Nature*. 1998;396:643-649.
2. Fukagawa T, Earnshaw WC. The Centromere: Chromatin Foundation for the Kinetochore Machinery. *Dev Cell*. 2014;30:496-508.
3. Blower MD, Daigle T, Kaufman T, et al. *Drosophila* CENP-A mutations cause a BubR1- dependent early mitotic delay without normal localization of kinetochore components. *PLoS Genet*. 2006;2:e110.
4. Tomonaga T, Matsushita K, Ishibashi M, et al. Centriomere protein H up-regulated in primary human colorectal cancer and its overexpression induces aneuploidy. *Cancer Res*. 2005;65:4683-4689.
5. Sun X, Clermont P-L, Jiao W, et al. Elevated expression of the centromere protein-A(CENP-A)-encoding gene as a prognostic and predictive biomarker in human cancers. *Int J Cancer*. 2016;139:899-907.
6. Amato A, Schillaci T, Lentini L, et al. CENPA overexpression promotes genome instability in pRb-depleted human cells. *Mol Cancer*. 2009;8:119.
7. Black BE, Cleveland DW. Epigenetic centromere propagation and the nature of CENP-a nucleosomes. *Cell*. 2011;144:471-479.
8. Wonsey DR, Follettie MT. Loss of the forkhead transcription factor FoxM1 causes centrosome amplification and mitotic catastrophe. *Cancer Res*. 2005;65:5181-5189.
9. Li Y, Zhu Z, Zhang S, et al. ShRNA-targeted centromere protein A inhibits hepatocellular carcinoma growth. *PLoS One*. 2011;6:e17794.
10. McGovern SL, Qi Y, Pusztai L, et al. Centromere protein-A, an essential centromere protein, is a prognostic marker for relapse in estrogen receptor-positive breast cancer. *Breast Cancer Res*. 2012;14:R72.
11. Qiu J-J, Guo J-J, Lv T-J, et al. Prognostic value of centromere protein-A expression in patients with epithelial ovarian cancer. *Tumour Biol*. 2013;34:2791-2795.
12. Hara M, Fukagawa T. Kinetochore assembly and disassembly during mitotic entry and exit. *Curr Opin Cell Biol*. 2018;52:73-81.
13. Perpelescu M, Fukagawa T. The ABCs of CENPs. *Chromosoma*. 2011;120:425-446.
14. Okada M, Cheeseman IM, Hori T, et al. The CENP-H-I complex is required for the efficient incorporation of newly synthesized CENP-A into centromeres. *Nat Cell Biol*. 2006;8:446-457.
15. Weir JR, Faesen AC, Klare K, et al. Insights from biochemical reconstitution into the architecture of human kinetochores. *Nature*. 2016;537:249-253.
16. Hori T, Okada M, Maenaka K, et al. CENP-O class proteins form a stable complex and are required for proper kinetochore function. *Mol Biol Cell*. 2008;19:843-854.
17. Minoshima Y, Hori T, Okada M, et al. The constitutive centromere component CENP-50 is required for recovery from spindle damage. *Mol Cell Biol*. 2005;25:10315-10328.
18. Hanissian SH, Akbar U, Teng B, et al. cDNA cloning and characterization of a novel gene encoding the MLF1-interacting protein MLF1IP. *Oncogene*. 2004;23:3700-3707.
19. Pan H-Y, Zhang Y-J, Wang X-P, et al. Identification of a novel cellular transcriptional repressor interacting with the latent nuclear antigen of Kaposi's sarcoma-associated herpesvirus. *J Virol*. 2003;77:9758-9768.
20. Kalitsis P, Fowler KJ, Earle E, et al. Targeted disruption of mouse centromere protein C gene leads to mitotic disarray and early embryo death. *Proc Natl Acad Sci USA*. 1998;95:1136-1141.
21. Fukagawa T, Brown WR. Efficient conditional mutation of the vertebrate CENP-C gene. *Hum Mol Genet*. 1997;6:2301-2308.
22. Howman EV, Fowler KJ, Newson AJ, et al. Early distribution of centromeric chromatin organization in centromere protein A (Cenpa) null mice. *PNAS*. 2000;97:1148-1153.
23. Okumura K, Kagawa N, Saito M, et al. CENP-R acts bilaterally as a tumor suppressor and as an oncogene in the two-stage skin carcinogenesis model. *Cancer Sci*. 2017;108:2142-2148.

24. Kagawa N, Hori T, Hoki Y, et al. The CENP-O complex requirement varies among different cell types. *Chromosome Res*. 2014;22:293-303.
25. Kemp CJ. Multistep skin cancer in mice as a model to study the evolution of cancer cells. *Semin Cancer Biol*. 2005;15:460-473.
26. Abel EL, Angel JM, Kiguchi K, et al. Multi-stage chemical carcinogenesis in mouse skin: fundamentals and applications. *Nat Protoc*. 2009;4:1350-1362.
27. Wilker E, Lu J, Rho O, et al. Role of PI3K/Akt signaling in insulin-like growth factor-1 (IGF-1) skin tumor promotion. *Mol Carcinog*. 2005;44:137-145.
28. Amornphimoltham P, Leelahavanichkul K, Molinolo A, et al. Inhibition of Mammalian target of rapamycin by rapamycin causes the regression of carcinogen-induced skin tumor lesions. *Clin Cancer Res*. 2008;14:8094-8101.
29. Brown K, Strathdee D, Bryson S, et al. The malignant capacity of skin tumours induced by expression of a mutant H-ras transgene depends on the cell type targeted. *Curr Biol*. 1998;8:516-524.
30. Kemp CJ, Donehower LA, Bradley A, et al. Reduction of p53 gene dosage does not increase initiation or promotion but enhances malignant progression of chemically induced skin tumors. *Cell*. 1993;74:813-822.
31. Matsumoto T, Jiang J, Kiguchi K, et al. Targeted expression of c-Src in epidermal basal cells leads to enhanced skin tumor promotion, malignant progression, and metastasis. *Cancer Res*. 2003;63:4819-4828.
32. Chan KS, Sano S, Kiguchi K, et al. Disruption of Stat3 reveals a critical role in both the initiation and the promotion stages of epithelial carcinogenesis. *J Clin Invest*. 2004;114:720-728.
33. Rundhaug JE, Gimenez-Conti I, Stern MC, et al. Changes in protein expression during multistage mouse skin carcinogenesis. *Mol Carcinog*. 1997;20:125-136.
34. Indra AK, Li M, Brocard J, et al. Targeted somatic mutagenesis in mouse epidermis. *Horm Res*. 2000;54:296-300.
35. Tomonaga T, Matsushita K, Yamaguchi S, et al. Overexpression and mistargeting of centromere protein-A in human primary colorectal cancer. *Cancer Res*. 2003;63:3511-3516.
36. Hanissian SH, Teng B, Akbar U, et al. Regulation of myeloid leukemia factor-1 interacting protein (MLF1IP) expression in glioblastoma. *Brain Res*. 2005;1047:56-64.
37. Li H, Zhang H, Wang Y. Centromere protein U facilitates metastasis of ovarian cancer cells by targeting high mobility group box 2 expression. *Am J Cancer Res*. 2018;8:835-851.
38. Vasioukhin V, Degenstein L, Wise B, et al. The magical touch: genome targeting in epidermal stem cells induced by tamoxifen application to mouse skin. *Proc Natl Acad Sci USA*. 1999;96:8551-8556.
39. Lichti U, Anders J, Yuspa SH. Isolation and short-term culture of primary keratinocytes, hair follicle populations and dermal cells from newborn mice and keratinocytes from adult mice for in vitro analysis and for grafting to immunodeficient mice. *Nat Protoc*. 2008;3:799-810.

SUPPORTING INFORMATION

Additional supporting information may be found online in the Supporting Information section.

How to cite this article: Saito M, Kagawa N, Okumura K, et al. CENP-50 is required for papilloma development in the two-stage skin carcinogenesis model. *Cancer Sci*. 2020;111:2850–2860. https://doi.org/10.1111/cas.14533